# FLUID FLOW THROUGH HAIR-BEARING APPENDAGES: FEEDING, SMELLING AND SWIMMING AT LOW AND INTERMEDIATE REYNOLDS NUMBERS

*M. A. R. KOEHL*

Department of Integrative Biology, University of California, Berkeley, CA 94720-3140, USA

## Summary

Many different types of animals use appendages bearing rows of hairs to capture food or molecules from the surrounding fluid, to locomote or to move fluids past themselves. The performance of these appendages, whose hairs operate at Reynolds numbers ($Re$) of $10^{-5}$ to 10, depends on how much of the fluid that they encounter flows through the gaps between the hairs rather than around the perimeter of the whole array. We have employed mathematical modeling, microcinematography of hairy appendages on small aquatic animals and flow visualizations around dynamically scaled physical models to elucidate the factors that determine the leakiness of arrays of hairs. We found that rows of hairs operating at very low $Re$ function as paddles, whereas those at $Re$ near 1 operate like leaky sieves. The $Re$ range through which the transition in leakiness occurs depends on the geometry of the appendage. We have discovered that different aspects of morphology and behavior are important in determining the leakiness of a hair-bearing appendage at different $Re$. Our study has revealed conditions under which morphological diversity of hairy appendages has little consequence for performance and other conditions under which simple changes in speed, size or mesh coarseness can lead to novel physical mechanisms of operation.

## Introduction

Many animals from different phyla use appendages bearing arrays of hairs to perform important biological functions such as feeding, gas exchange, olfaction and locomotion. For example, a wide variety of suspension-feeding animals employ devices composed of rows of hairs (Fig. 1A, see Fig. 6) to separate food particles from the water around them. Other hair-bearing structures, such as olfactory antennae (Fig. 1B) and filamentous gills (Fig. 1C), capture molecules from the surrounding air or water. Many small animals also use hairy appendages to swim or fly through fluids (Fig. 1D,E) or to produce respiratory or feeding currents (see Fig. 5A). As these examples illustrate, arrays of hairs are important not only because they serve a variety of essential biological functions, but also because they are found in so many different taxa. (Unfortunately, the nomenclature for such hairs and for the appendages that bear them is taxon-specific. For ease of discussion, I will simply refer to them all as 'hairs' or 'bristles' on 'appendages' or 'legs', and I will only indulge in jargon when referring to particular species.)

kinematics. The purpose of this paper is to summarize what we have learned thus far about how the structure and motion of a hair-bearing appendage can affect fluid flow.

## Importance of fluid flow near hairs in an array

Most of the types of hairs listed above operate at Reynolds numbers of the order of $10^{-5}$ to 10 (e.g. reviewed by Rubenstein and Koehl, 1977; LaBarbera, 1984; Cheer and Koehl, 1987a; Shimeta and Jumars, 1991; Loudon *et al.* 1994). Reynolds number ($Re=UL/\nu$, where $U$ is velocity, $L$ is a linear dimension, in this case hair diameter, and $\nu$ is the kinematic viscosity of the fluid) represents the ratio of inertial to viscous forces for a particular flow situation. At the low and intermediate $Re$ at which these hairs operate, viscosity is very important in determining flow patterns, although inertia cannot be ignored for hairs operating at the upper end of this $Re$ range. When a viscous fluid flows over a solid surface (such as the surface of a hair), the layer of fluid in contact with the surface does not slip relative to the surface and a velocity gradient develops in the fluid between the object and the freestream flow. The same is true for a body moving through a stationary fluid: some fluid sticks to and moves along with the body, and a velocity gradient develops in the fluid around the object. The lower the $Re$, the thicker this layer of sheared fluid is relative to the dimensions of the body. If the layers of fluid moving along with the hairs in an array are thick relative to the gaps between the hairs, then little fluid may leak through the array.

How much fluid flows through the gaps between hairs on a hair-bearing appendage? We have defined the 'leakiness' of such a gap as the ratio of the volume of fluid that flows through the gap in a unit of time to the volume of fluid that would have flowed (at freestream velocity) through a space of that width if there were no hairs present (Fig. 2) (Cheer and Koehl, 1987a). Fluid moves around rather than through a hair-bearing appendage with low leakiness; hence, the appendage is functionally a paddle. In contrast, a hair-bearing appendage with a high leakiness functions like a sieve. Futhermore, at a given speed of appendage motion (i.e. at a given freestream velocity relative to the appendage), the velocity gradient next to a hair in a leaky appendage is steeper than that next to a hair in a non-leaky array (Cheer and Koehl, 1987a; Loudon *et al.* 1994).

The performance of various functions by hair-bearing appendages depends on their leakiness. For example, the amount of water that sticks to and moves with a raptorial appendage determines whether an organism can use that appendage to reach out and grab a food item without pushing it away (Koehl and Strickler, 1981). The effectiveness of a suspension-feeding appendage that filters particulate matter (such as single-celled algae, bacteria or organic particles) from the water also depends on flow through the appendage in several ways: the volume of fluid that can be filtered per unit of time depends on the leakiness of the array of hairs, and the percentage of particles of various physical characteristics that is captured from that volume of fluid depends on the velocity gradients near individual hairs (as described in, for example, Rubenstein and Koehl, 1977; Shimeta and Jumars, 1991). In a similar way, leakiness affects the flux of molecules to the surfaces of hairs in gills and olfactory antennae (e.g. Berg and Purcell, 1977; Murray, 1977;
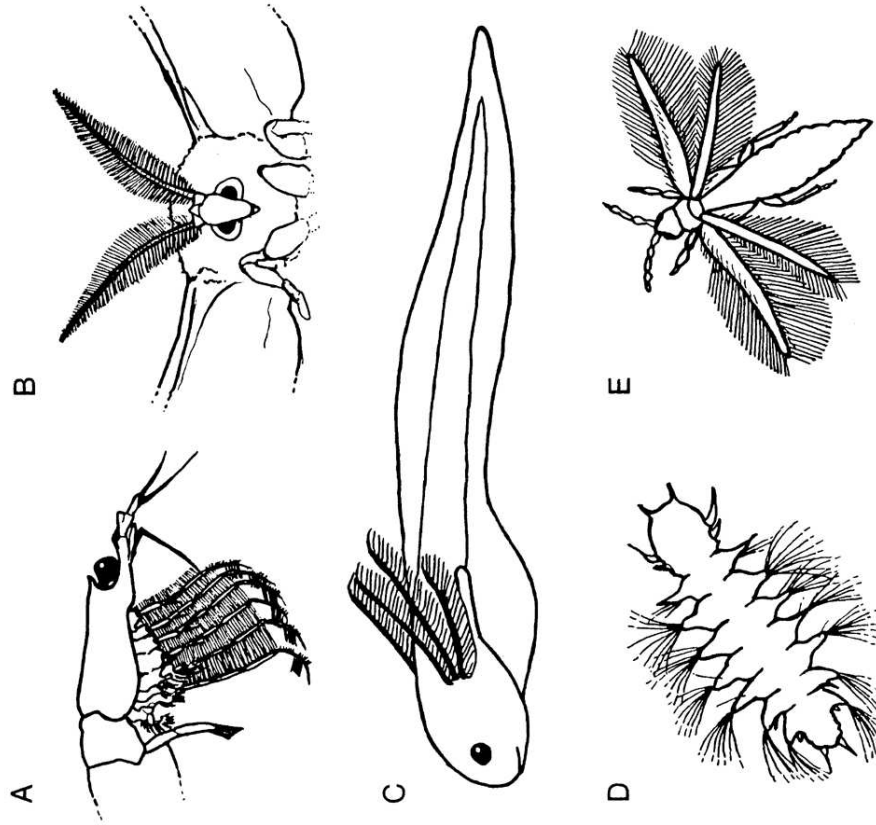


Fig. 1. Examples of hair-bearing appendages that serve different functions: (A) Suspension-feeding legs of a euphausid ('krill'), Phylum Arthropoda; (B) olfactory antennae of a male moth, Phylum Arthropoda; (C) external gills of a larval African lungfish, Phylum Chordata; (D) swimming parapodia of a nereid larva, Phylum Annelida; (E) wings of a thrips, Phylum Arthropoda.

To perform any of the functions listed above, an array of hairs must interact with the water or air around it. Therefore, the first step in figuring out how such an array works is to determine how fluid moves with respect to the hairs when an animal uses the appendage. If we want to move beyond analyses of the mechanisms by which specific appendages of particular organisms work, however, to address broader ecological or evolutionary questions, then we must also ask in more general terms how the performance of an array of hairs depends on defined aspects of its morphology and

$$\text{``leakiness''} = \frac{\left(\begin{array}{c}\text{volume that actually}\\ \text{flows through gap}\end{array}\right)}{\left(\begin{array}{c}\text{volume that would flow}\\ \text{through gap if cylinders}\\ \text{were not there}\end{array}\right)}$$
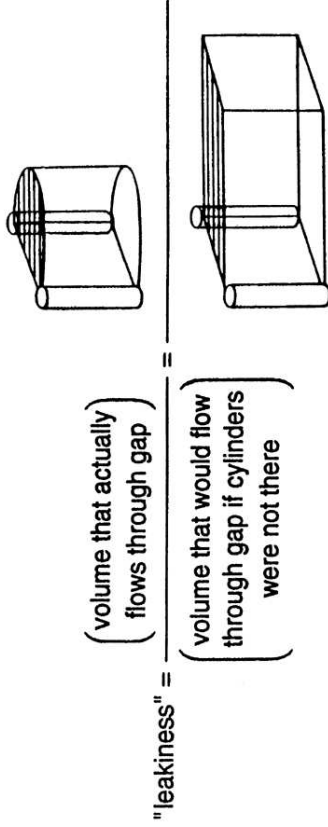
Fig. 2. Leakiness is the ratio of the volume of fluid that actually flows through the gap between a pair of cylinders of unit length in a unit of time (upper diagram) to the volume of fluid that would have flowed through the same area in that unit of time if the cylinders had not been there (i.e. the volume of space between the cylinders across which they sweep in that unit of time; lower diagram) (Cheer and Koehl, 1987a).

Schmidt and Ache, 1979; Futrelle, 1984; Atema, 1985; Moore et al. 1991). Moreover, the leakiness of hairy locomotory appendages has been assumed to determine their effective area for generating lift and thrust (e.g. Ellington, 1975; Morris et al. 1990). Indeed, Leonard (1992) has measured lower drag on arrays of cylinders (at $Re$, based on cylinder diameter, of about 2–200) than on solid plates.

I will use leakiness as a general measure of appendage performance in this paper in order to explore the consequences of morphology and kinematics. Obviously, analyses of particular functions (such as feeding or swimming) should use more relevant measures of performance (e.g. capture rate or cost of transport).

## Approaches to studying the fluid flow through arrays of hairs

The flow between hairs can be studied using various empirical and theoretical tools, each with particular advantages and limitations.

First, we can use mathematical models to express quantitatively our theories about the mechanisms underlying a process or to describe quantitatively the behavior of a system. Such models enable us to predict the effects on performance of varying defined parameters, and they also permit us to study combinations of morphology and behavior not found in nature. However, with mathematical models, we are limited to relatively simple geometries and kinematics. Although numerical models run on today's high-speed computers permit us to describe ever more complex systems, they can become very cumbersome and time-consuming.

Second, we can measure the kinematics of, and forces on, real organisms as well as the fluid velocities around them, although many of the technical challenges of doing so for rapidly moving microscopic organisms have not yet been solved. Unfortunately, the diversity available in nature limits our ability to investigate the consequences of

particular aspects of morphology or behavior: we cannot systematically vary one parameter while holding all others constant to quantify the effects of each.

Third, we can measure fluid motion around and forces on dynamically scaled physical models. Flow situations characterized by the same geometry and $Re$ are dynamically similar; hence, the ratios of velocities and forces at analogous points in the fluid around a model and a prototype, both operating at a given $Re$, are the same. Therefore, a large model moved at a conveniently slow speed in viscous syrup can be used to study the fluid dynamics of a microscopic appendage operating at the same $Re$ in water or air. Repeatable velocity and force measurements that cannot be made on uncooperative, delicate microscopic organisms are technically possible with large models. Furthermore, greater spatial and temporal resolution of such measurements can be achieved with large, slow models than is possible with small organisms. Like mathematical models, dynamically scaled physical models have the advantage that parameters can be varied one at a time as the investigator chooses, and combinations that do not exist in nature can be tried. Such physical models, however, can be more complicated in geometry and behavior than is practical for mathematical models. Of course, as with mathematical models, physical models are only as good as their underlying assumptions.

## Mathematical models of flow between hairs

### Models of flow through filters

Reviews of methods that have been used to calculate fluid motion through mesh-like structures can be found in the literature on filters (e.g. Fuchs, 1964; Davies, 1973; Laws and Livesey, 1978). For example, the two-dimensional flow at low $Re$ through an infinite row of cylinders has been modeled (Tamada and Fujikawa, 1957). Since all the fluid must flow through the gaps between hairs in an infinite array, a decrease in gap width leads to an increase in velocity between the hairs. Obviously, such models are not appropriate for hair-bearing legs of finite width since fluid can flow around as well as through such appendages.

One approach to estimating the flow through mesh-like structures of finite width is to treat them like porous plates. Various methods of calculating flow through and around porous screens submerged in a fluid are given by Taylor and Batchelor (1949), Spielman and Goren (1968) and Koo and James (1973). The resistance to flow through biological filters has been estimated using Darcy's law (Cheer and Koehl, 1987a) or using a modification of Tamada and Fujikawa's model (Silvester, 1983). Unfortunately, Darcy's law yields leakiness values for various insect filters that are orders of magnitude too low when compared with empirical data (Cheer and Koehl, 1987b). The predictions of Silvester's model agree reasonably well with water flow measured through the silk feeding nets spun by aquatic caddisfly larvae (Loudon, 1990), but underestimate flow through feathery moth antennae (by about 50%) and through feeding fans of aquatic black fly larvae (by several orders of magnitude) (Cheer and Koehl, 1987b). Thus, it appears that modeling biological structures composed of rows of hairs as porous screens is only valid when the morphology of the array approximates that of a screen (i.e. when the hairs in a row bear bristles that completely span the gaps between adjacent hairs). A

much better match with empirical measurements of flow through hairy appendages has been achieved by the modeling approach of Cheer and Koehl (1987a,b).

### Model of flow between a pair of cylinders

Cheer and Koehl (1987a) used a two-dimensional analytical model to calculate fluid movement between and around a pair of circular cylinders at low $Re$. Flow velocities near the hairs were calculated in bipolar coordinates using Stoke's low-$Re$ approximation of the Navier–Stokes equations, and flow velocities far from the hairs were calculated in polar coordinates using Oseen's low-$Re$ approximation (which takes inertial effects into consideration). A matched asymptotic expansion technique was used to put these two flow fields together.

We used the velocity profiles predicted by this model to determine the leakiness of pairs of hairs operating at a variety of biologically relevant $Re$ and spacings. (Throughout this paper, $Re$ is based on hair diameter and spacing is represented as the ratio of gap width to hair diameter, $G/D$.) Our results (Fig. 3) provide several insights about the functional morphology of hair-bearing appendages.

The leakiness of a pair of hairs depends on $Re$. At $Re$ near 1, little fluid is dragged along with the hairs as they move, and a hairy appendage should be sieve-like. In contrast, at very low $Re$, little fluid moves through the gap between adjacent hairs, and a hair-bearing leg should behave more like a paddle. What happens if an organism changes its $Re$ (i.e. it grows or changes its speed of appendage motion)? Such a change has little effect on leakiness at very low $Re$ ($\leq 10^{-3}$); hence, there is great scope in this low-$Re$ range for variation in size or behavior without consequences to leakiness. (Of course, increasing speed increases the volume flow rate through an appendage and the steepness of the velocity gradients next to hairs, even if the leakiness of the appendage is unchanged by such a behavioral modification.) In contrast, a change in $Re$ in the range between $10^{-2}$ and 1 produces a substantial change in leakiness and hence in the operation of the appendage as a sieve versus as a paddle.

What happens to leakiness if the spacing between adjacent hairs is changed? At a $Re$ of $10^{-1}$ and $10^{-2}$, there is a pronounced reduction in leakiness as hairs are moved closer together. At a $Re$ of 0.5, however, such a reduction in leakiness only occurs when the hairs are already very close together; there is no effect on leakiness of changing the spacing at a gap:diameter ratio of approximately 15 or greater. At very low $Re$ ($\leq 10^{-3}$), gap width also has little effect on leakiness. Thus, we see again that there is scope for morphological variation at these very low Reynolds numbers with little consequence to leakiness.

### Numerical model of flow through arrays of hairs

The model described in Cheer and Koehl (1987a) only deals with two cylinders at $Re<1$, whereas most hairy appendages bear more than two hairs and some animals operate their hairs at $Re>1$. Therefore, Abdullah and Cheer (unpublished results; described in Koehl, 1993) used a numerical model to compute the steady, two-dimensional flow near cylinders at $Re$ between 0.5 and 4 to investigate the consequences
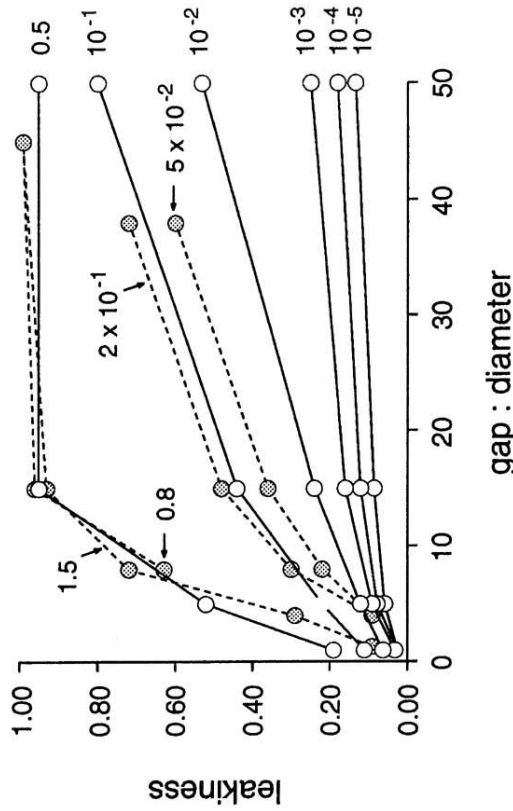
Fig. 3. Plot of leakiness (defined in Fig. 2) as a function of gap:diameter ratio of neighboring hairs. Open circles and solid lines represent the leakiness calculated using the model of Cheer and Koehl (1987a). Grey circles and dashed lines represent leakiness measured during towing experiments with the comb-like physical models of Hansen and Tiselius (1992) (see Fig. 8D). Each line represents a different $Re$, as indicated by the numbers near the lines.

of adding more cylinders to a row. Their results have several intriguing biological implications (Koehl, 1993).

As $Re$ increases above 1, Abdullah and Cheer's model predicts that the shapes of the velocity profiles between hairs become irregular, with velocity peaks near the cylinders exceeding the freestream velocity (e.g. Fig. 8 in Koehl, 1993). Since the flux of particles or molecules to the capturing surfaces of the hairs on filter-feeding appendages, gills and olfactory antennae is a function of the steepness of the velocity gradients adjacent to the hairs (e.g. Rubenstein and Koehl, 1977; Shimeta and Jumars, 1991; Murray, 1977; Futrelle, 1984), a small change in the speed of a row of hairs operating at $Re$ around 1 might make a big difference to its performance.

Abdullah and Cheer's model predicts that the addition of more hairs to a row reduces leakiness if $Re<1$, but increases leakiness if $Re>1$, and measurements of flow through physical models have shown the same phenomenon (Fig. 4). These results suggest that a simple morphological change (a change in the number of hairs on an appendage) can have *opposite* consequences at slightly different $Re$. Although this observation is intriguing,
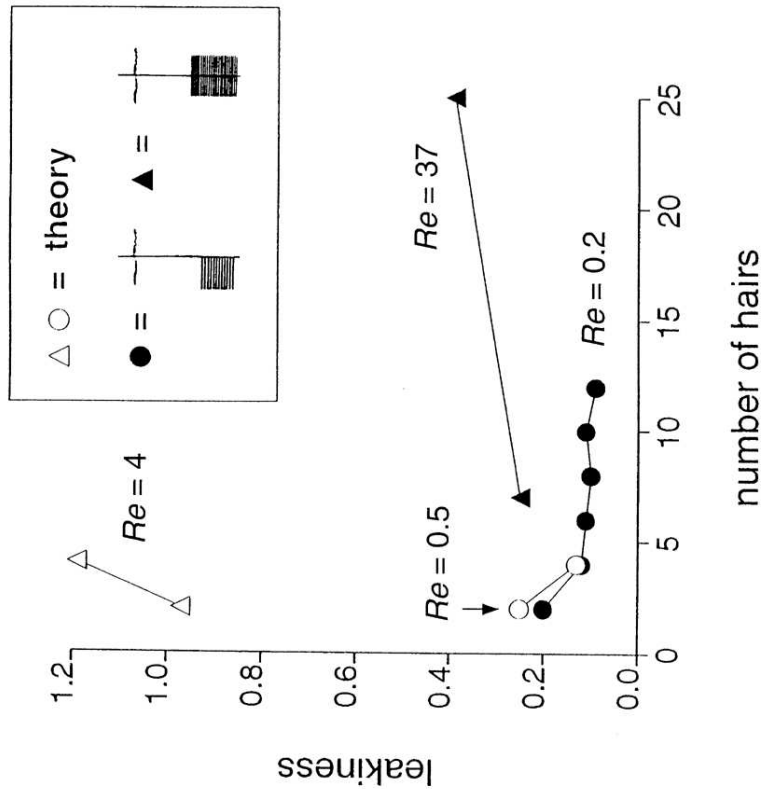
structures perform a function of tremendous ecological importance, but also because they provide a diversity of morphologies and Reynolds numbers to compare.

Calanoid copepods (Fig. 5A) are small planktonic crustaceans (body lengths of millimeters) than can be extremely abundant in oceans and lakes. Most of these planktonic copepods, which are among the most numerous multicellular animals on earth, feed on unicellular algae and other suspended particulate matter, forming a major link in many aquatic food webs (e.g. Russell-Hunter, 1979; Ruppert and Barnes, 1994). Because of the ecological importance of copepod feeding, many investigators have studied it, often focusing on the rates at which copepods remove various kinds of particles from the water (reviewed in Koehl, 1984). In spite of all this attention, the mechanisms by which copepods capture particulate food were not understood. Textbooks described a specific pair of appendages, the second maxillae (M2s), as filters that strain particles from a current of water forced through them by the beating of four other pairs of feeding legs (reviewed by Koehl, 1984) (Fig. 5A). The M2s, which are composed of hairs ('setae') bearing smaller hairs ('setules'), do indeed look like filters (Fig. 6).

The first step in analyzing copepod feeding was to work out the kinematics of their appendages during feeding and to try to determine the velocity of water flow through the filters (the M2s) when the animals capture different types of particles. Making such measurements posed a number of technical challenges: (1) a copepod is so small that it must be viewed with a microscope, but the flow it creates cannot be studied if the animal is confined to a drop of water on a microscope slide, and (2) a copepod flaps its feeding appendages at such high frequencies that high-speed cinematography is necessary to resolve their motions. Fortunately, Strickler developed an optical system that permitted high-speed microcinematography of zooplankton in large containers of water (e.g. Alcaraz et al. 1980). By marking water near feeding copepods with dye released from a micropipette, we were able to use such a system to record water and appendage motions during feeding by several species of copepods (Koehl and Strickler, 1981; Koehl, 1981, 1983, 1993; Koehl et al. 1984, and unpublished data).

We discovered that the water current produced by the four pairs of feeding appendages bypasses the M2s; rather than being passive filters, the M2s actively capture food particles from this scanning current (Koehl and Strickler, 1981). During a capture, the M2s fling away from each other (Fig. 5B,C) and then squeeze back together (Fig. 5D,E), as described by Koehl and Strickler (1981). Other microcinematographic studies of the feeding behaviors of copepods have revealed variations in the M2 motions used by different species to capture, manipulate or reject particles (e.g. Alcaraz et al. 1980; Paffenhöfer et al. 1982; Cowles and Strickler, 1983; Price et al. 1983; Price and Paffenhöfer, 1984, 1986; Strickler, 1984; Vanderploeg and Paffenhöfer, 1985). For example, some species use a single fling-and-squeeze to capture large particles, but a series of low-amplitude fling-and-squeeze motions to pump small particles towards the mouth (Price and Paffenhöfer, 1986).

To explore the fluid-mechanical consequences of such differences in M2 motion, we have filmed dye streams around five species of copepods whose M2s differ in speed and in mesh coarseness (examples of three species are shown in Fig. 6) (Koehl et al. 1984, and unpublished data; Koehl, 1993). Frame-by-frame analysis of these movies of feeding



Fig. 4. Leakiness plotted as a function of hair number. Triangles represent $Re > 1$ and circles represent $Re < 1$. Open symbols are based on calculations of Abdullah and Cheer (cited in Koehl, 1993) and filled symbols are based on measurements for comb-like models (filled triangles, Leonard, 1992; Fig. 8C; filled circles, Hansen and Tiselius, 1992; Fig. 8D).

we must investigate the consequences of hair number over a wider range of $Re$ and for arrays bearing more hairs than have thus far been studied before we can speculate about the biological importance of hair number to appendage performance.

While general models such as those described above can point out basic rules about how morphology and behavior ought to affect the performance of hair-bearing appendages, we must turn to real animals to test these ideas.

## Measurements of flow through hair-bearing appendages of organisms: second maxillae of calanoid copepods

As described in the Introduction, nature offers a vast array of hairy legs from which to choose study systems to test predictions of the models described above. We have focused on the food-capturing appendages of calanoid copepods, not only because these

copepods permitted us to measure the velocities and spacings of the setae on the M2s when the animals captured different sorts of food. We also conducted a morphometric analysis of the second maxillae of these species. Such measurements revealed that the setae on the second maxilla of copepods operate at $Re$ ranging from $10^{-2}$ to 1. Recall that this is the $Re$ range in which theory predicts a transition between being a paddle and being a sieve. How leaky are these second maxillae?

We used the model of Cheer and Koehl (1987a) to calculate the leakiness of the M2s of various species of copepods (Koehl, 1993; M. A. R. Koehl and A. Y. L. Cheer, unpublished data). The velocity profiles around a seta with a neighbor were calculated for various positions along the length of an M2. Using these velocities as the freestream

velocities encountered by the setules, the velocity profiles between pairs of setules were then calculated and used to determine leakiness. These calculations predicted that some species of copepods, such as *Centropages furcatus* (Fig. 6A), whose setae operate at an $Re$ of the order of 1, should function like leaky sieves. In contrast, they predicted that other species, such as *Eucalanus pileatus* (Fig. 6B) and *Temora stylifera* (Fig. 6C), whose setae operate at an $Re$ of the order of $10^{-2}$, should function like non-leaky paddles.

Are these predictions consistent with observations of water flow near second maxillae? If we look at what happens to fine dye streaks in the water when copepods move their second maxillae through them, we do indeed see that the dye flows readily between the setae of *C. typicus* M2s, but moves only slightly between the setae of *E. pileatus* or *T. stylifera* M2s (Koehl, 1993). What mechanisms can appendages characterized by such different leakinesses use to capture particles?

Microcinematography of the motion of particles and dye near the M2s of feeding copepods has revealed two basic types of food capture mechanisms. (1) M2s whose setae operate at an $Re$ of the order of 1 during a fling and squeeze filter particles from the water during the squeeze (Koehl, 1993; M. A. R. Koehl and G.-A. Paffenhöfer, unpublished data). (2) M2s whose setae operate at an $Re$ of the order of $10^{-2}$ capture particles by moving the water surrounding the particles. When capturing a particle using a single low-$Re$ fling and squeeze, a parcel of water containing the particle is drawn between the M2s during the fling, as described by Koehl and Strickler (1981). When feeding on very small particles by repeatedly flapping the M2s apart and together at low $Re$ (Price and Paffenhöfer, 1986), a slowly moving stream of fluid carries the particles towards the mouth. [Childress *et al.* (1987) have modeled various mechanisms by which such appendage motions near a body surface can produce net flow at low $Re$]. These M2s from different species of copepods provide an example of hairy appendages that qualitatively execute similar motions (they fling apart and squeeze together to catch particles), but that capture particles by different physical mechanisms simply because the $Re$ at which they move falls on either side of the transition between paddle-like and sieve-like behavior.

*Quantitative comparison of model predictions with measured leakinesses of M2s*

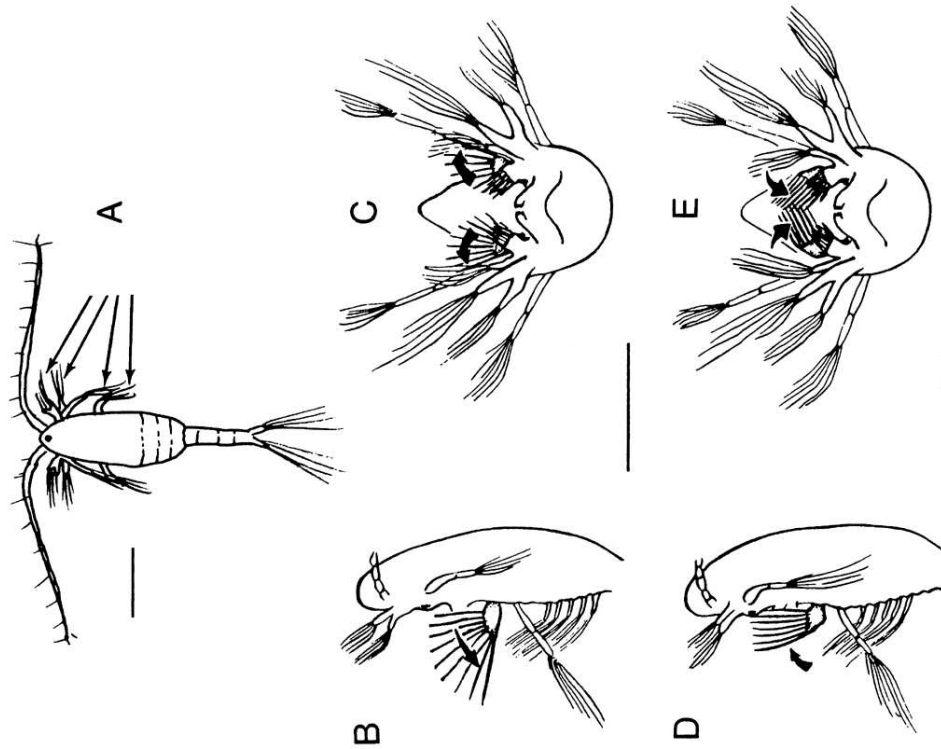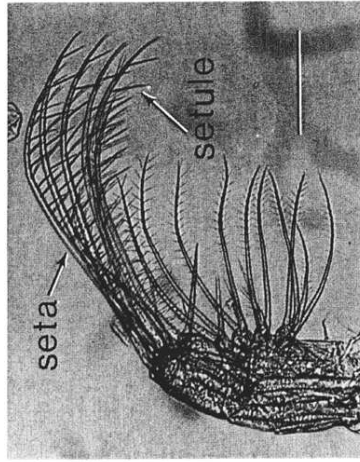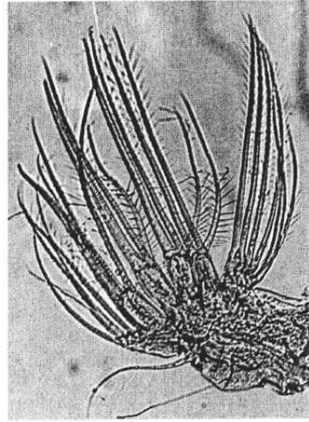Although our model's predictions of which M2s operate as filters and which as paddles



Fig. 5. Diagrams of a calanoid copepod. (A) Dorsal view of a copepod with its anterior end towards the top of the page. Arrows indicate the four pairs of hairy appendages that produce the feeding current past the animal (second antennae, mandibular palps, first maxillae and maxillipeds), as described in Koehl and Strickler (1981). The food-capturing second maxillae (M2s) (see Fig. 6) and the swimming legs are on the ventral side of the animal and are not visible in this view. Scale bar, 0.25 mm. (B) Lateral view of a copepod flinging its M2s apart from each other and away from the body surface. The black arrow indicates the direction of motion of the left M2. The first maxillae have been omitted from the diagram so that the motion of the M2 could be shown. Scale bar, 0.25 mm for B–E. (C) Head-on view of a copepod flinging its M2s. The ventral surface of the animal is facing the top of the page. Black arrows indicate the directions of motion of the two M2s. The large first antennae have been omitted from the diagram. (D) Lateral view of a copepod squeezing its M2s back together and towards the body. (E) Head-on view of a copepod during an M2 squeezing motion (B–D are based on descriptions in Koehl and Strickler, 1981).
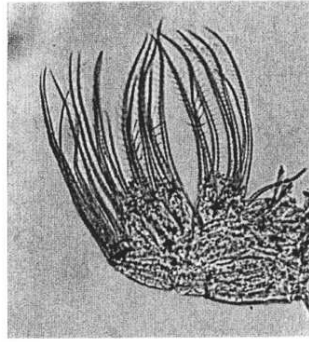
Fig. 5

# SECOND MAXILLAE (M2)

seta

setule



*Centropages furcatus*
Re = 1

*Eucalanus pileatus*
Re = 10$^{-2}$ to 10$^{-1}$

*Temora stylifera*
Re = 10$^{-2}$

Fig. 6. Light micrographs of the particle-capturing second maxillae (M2s) of several of the species of calanoid copeods we have studied. M2s are composed of large hairs (setae) bearing smaller bristles (setules). The Reynolds numbers (*Re*) reported under each figure indicate the order of magnitude of the *Re* at which the setae operate (based on the diameters and velocities of the distal quarter of the setae). Scale bar, 0.1 mm.

are consistent with observations of dye movements on films of real copepods, our quantitative predictions of leakiness should be compared with those measured through real hair-bearing appendages. Few measurements have been made of the leakiness of
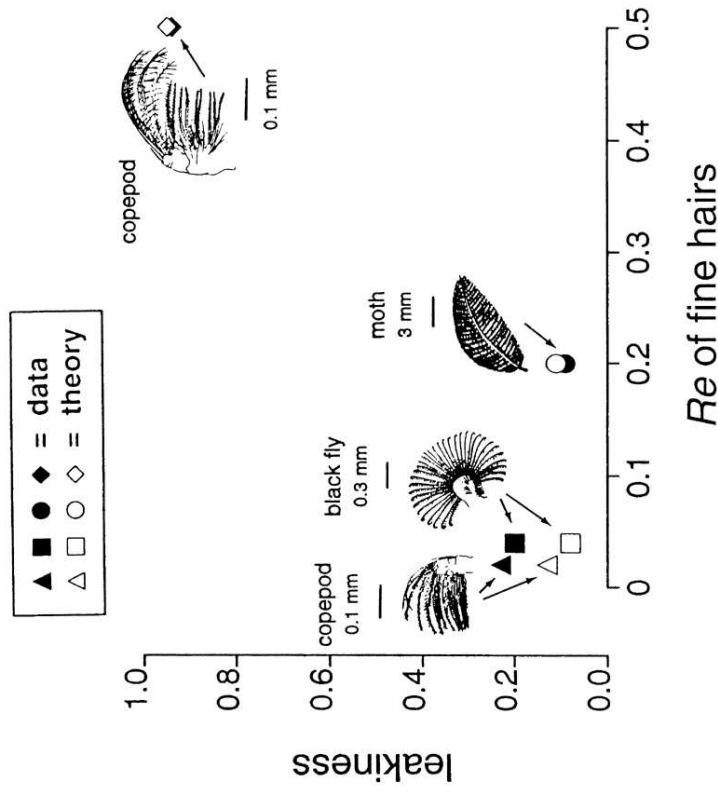
Fig. 7. Leakiness of various hairy appendages plotted as a function of the *Re* of the finest hairs in the mesh of each. Filled symbols represent leakiness measured through real appendages and open symbols represent leakiness calculated using the model of Cheer and Koehl (1987*a*). Triangles, suspension-feeding M2s of the copepod *Eucalanus pileatus* (data and theoretical results from Koehl, 1993); squares, suspension-feeding fans of the aquatic larva of a black fly *Similium vittatum* (data from Craig and Chance, 1982; theoretical results from Cheer and Koehl, 1987*b*); circles, antenna of a male moth *Acitas luna* (data from Vogel, 1983; theoretical results from Cheer and Koehl, 1987*b*); diamonds, suspension-feeding M2s of the copepod *Centropages furcatus* (data and theoretical results from Koehl, 1993).

hair-bearing animal appendages, but the data available are shown in Fig. 7, where they are compared with predictions made using our model. Our predictions for hairs operating at *Re* of 10$^{-1}$ to 1 are in very close agreement with empirical measurements. In contrast, at lower *Re*, the real appendages are leakier than our model predicts. This tells us that there are features of these hairy appendages that affect their leakiness at low *Re* but that we have not incorporated into our model. For example, our model considers hairs in an unbounded fluid, whereas real appendages beat in proximity to the body of the animal to which they are attached. Furthermore, our model is two-dimensional, whereas hairs on real appendages are of finite length and experience three-dimensional flow. As we move to more complicated motions and geometries, it becomes more practical to investigate
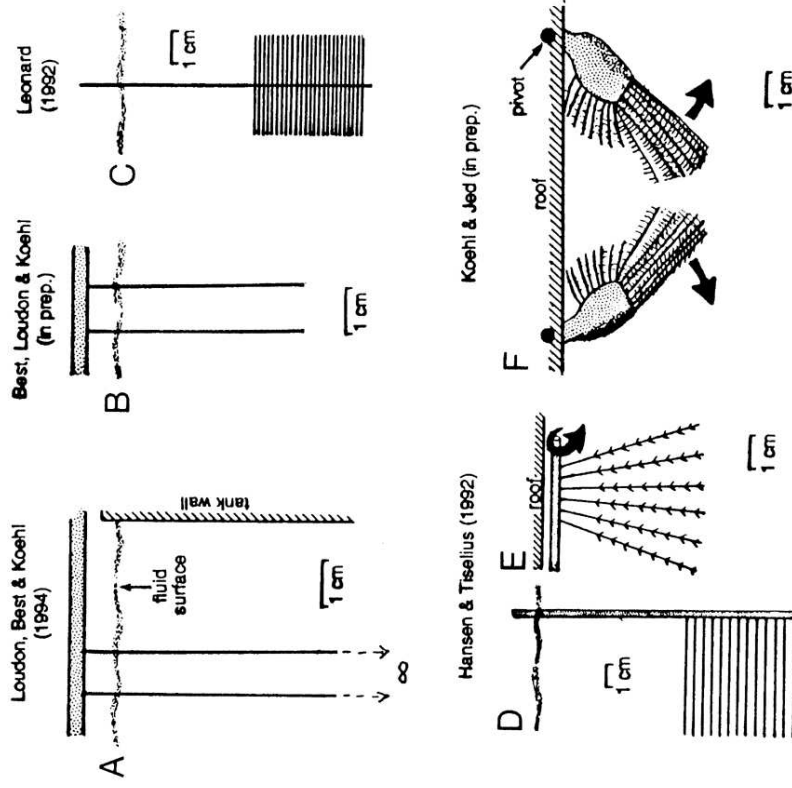
Fig. 8. Diagrams of some of the physical models that have been used to study flow through hair-bearing appendages. (A) Loudon et al. (1994) towed pairs of cylinders (which could be compared with the model of Cheer and Koehl, 1987a) at steady velocities through a tank of corn syrup solutions. We used 'infinitely long' cylinders (that extended from the floor of the tank to the top of the fluid) to explore the consequences of moving near walls. (B) B. A. Best, C. Loudon and M. A. R. Koehl (in preparation) also towed pairs of cylinders at steady velocities through the same tank to explore the consequences of cylinder length and gap width. (C) Leonard (1992) towed comb-like models at steady velocities through a tank of water or magnesuim sulphate solutions. (D) Hansen and Tiselius (1992) towed comb-like models at steady velocities through a tank of glycerol solutions. (E) Hansen and Tiselius (1992) also rotated in their tank various models of an appendage with six hairs. (F) M. A. R. Koehl and J. Jed (in preparation) used scale models of pairs of M2s from particular species of copepods (Fig. 6). These models executed fling-and-squeeze motions in mineral oil near a roof simulating a copepod body surface.

flow using dynamically scaled physical models rather than very cumbersome numerical models.

### Dynamically scaled physical models

A variety of physical models have been used to investigate the fluid motion near hair-bearing appendages (Fig. 8). These models range from simple pairs of cylinders (that can be directly compared with our mathematical model) and comb-like models towed at steady speeds, to more realistic replicas of appendages flapped near walls representing body surfaces. Leakiness was measured in some of these model studies, whereas qualitative observations of flow around or through the models were reported in other studies. I have digitized (using a Jandel digitizing tablet no. 2210 and SigmaScan 3.9 software) the data for comb-like models given in Fig. 6 of Hansen and Tiselius (1992) and in Figs 15 and 16 of chapter 5 in Leonard (1992) so that I could replot their leakiness values along with ours to address various questions posed below.

*What are the consequences of moving relative to nearby walls?*

We explored the consequences of moving hairs relative to nearby walls (such as the body surface of an animal, the wall of a burrow or the substratum in an animal's habitat) by measuring the leakiness of pairs of cylinders moved along or towards the walls of an aquarium (Fig. 8A) (Loudon et al. 1994) and comparing these values with those calculated for pairs of cylinders in an unbounded fluid (Cheer and Koehl, 1987a).

We found (Loudon et al. 1994) that at a $Re$ of $10^{-2}$ and lower, the leakiness of a pair of cylinders moving through fluid in a tank with walls was higher than that predicted by Cheer and Koehl (1987a) for cylinders in an unbounded fluid, even when the cylinders were far away (70 diameters) from the nearest wall. We also found that a change in gap:diameter ratio ($G/D$) could affect the leakiness of a pair of cylinders moving relative to a wall (Loudon et al. 1994), whereas Cheer and Koehl (1987a) predicted no effect of $G/D$ for cylinders operating at such low $Re$ in an unbounded fluid. Therefore, a morphological character (i.e. $G/D$) that is of little consequence at low $Re$ in an unbounded fluid becomes important when the appendage operates near a wall. We also found that when cylinders operated at $Re \leqslant 10^{-2}$, leakiness could be increased by moving very close (less than 15 diameters) to a wall (Loudon et al. 1994). Although motion at low $Re$ relative to a wall also increased the leakiness of cylinders at great distances from the wall, changes in distance from the wall did not alter leakiness significantly once the cylinders were farther than about 15 diameters from the wall.

Although we measured pronounced wall effects at very low $Re$, we found that the leakiness of the physical models moving near walls at $Re$ of $10^{-1}$ and 1 matched the theoretical values for cylinders in an unbounded fluid. This suggests that a behavior that is effective at altering leakiness at very low $Re$ (i.e. moving close to the body surface or another wall), does not change leakiness at intermediate $Re$.

Our observations about wall effects on leakiness point out some practical considerations for those of us studying flow through hairy appendages. At $Re \leqslant 10^{-2}$,

assuming an unbounded fluid when modeling an appendage that moves relative to an animal's body will result in underestimation of flow velocities through the appendage. Furthermore, at these low values of $Re$, the walls of the tank in which physical models are

moved will increase the fluid motion relative to the models. (Note that we have focused on the case of a hair-bearing appendage moving *relative to* a wall. Of course, if a hair is attached to a wall and both move together – or both are stationary in an ambient current – then the wall effect is the opposite of what we have reported: the wall reduces the velocity relative to the hair, which stands partially or fully within the boundary layer of slowed fluid along the surface of the wall.)

### What are the consequences of hair length?

The mathematical model of Cheer and Koehl (1987a,b) is two-dimensional, and the physical models of Loudon et al. (1994) are of infinitely long cylinders (i.e. they extend from the bottom of the tank through the surface of the fluid; Fig. 8A); hence, neither study addresses the consequences of fluid flowing around the tips of hairs of finite length. B. A. Best, C. Loudon and M. A. R. Koehl (in preparation) used physical models of pairs of hairs to study the consequences of hair length to leakiness (Fig. 8B). Our results indicate that the leakiness of the gap between cylinders operating at $Re \leq 10^{-2}$ is lower if the cylinders are of finite length (Fig. 9) because fluid is free to flow around the tips of the appendage as

well as around the sides. In contrast, when models are quite leaky ($Re=1$), we found no difference in the flow between hairs of finite or infinite length. Our data for pairs of cylinders of finite length show no significant effect on leakiness of changing cylinder length. In contrast, the data of Hansen and Tiselius (1992) for comb-like models (Fig. 8D) indicate that increasing hair length:diameter ratio can decrease comb leakiness (Fig. 9).

### What are the consequences of hair Reynolds number?

The results of a variety of physical model studies are consistent with our prediction that a row of hairs operating at $Re \leq 10^{-2}$ is paddle-like whereas one moving at a $Re$ of the order of 1 is sieve-like. For example, Gerritsen and Porter (1982) found that no dye passed through their models (plankton netting oscillating in glycerine) of cladoceran feeding appendages whose setules operate at an $Re$ of $10^{-3}$ to $10^{-4}$. Braimah (1987) towed through canola oil scale models of three of the microtrichia-bearing rays (i.e. bristle-bearing cylinders) from the filter-feeding forelegs of larval mayflies and labral fans of larval black flies. He found virtually no flow between the bristles at a bristle $Re$ of 0.02 to 0.07, but increasingly thinner boundary layers and greater flow through the models as bristle $Re$ was raised to 0.8. Similarly, Hansen and Tiselius (1992) used six bristle-bearing cylinders rotated in mixtures of glycerol and water to model a copepod M2 (Fig. 8E). At a $Re$ of the order of $10^{-2}$, they observed dye to flow through the models only at the very tips of the cylinders, whereas at $Re \geq 1$, they saw dye move through the models all along the length of the cylinders.

### What are the consequences of mesh gap:diameter ratio?

Hansen and Tiselius (1992) used comb-like models (Fig. 8D) towed at steady velocities to explore the the leakiness consequences of cylinder spacing. At an $Re$ where the wall effects of the towing tank are not expected to affect leakiness, these comb-like models showed leakinesses very similar to those predicted by Cheer and Koehl (1987a) (Fig. 3), the main difference being lower-than-predicted leakinesses at very low values of $G/D$. (The latter may be due to fluid motion around the tips of the hairs in the three-dimensional models, as well as to the additional resistance of the support rod to fluid motion between the hairs.)

Leonard (1992) and Hansen and Tiselius (1992) tested comb-like models (Fig. 8C,D) at $Re$ higher than those at which the model of Cheer and Koehl (1987a) is applicable. As illustrated in Fig. 10A, the critical $G/D$ (the $G/D$ below which gap width affects leakiness) becomes lower as $Re$ is increased. Similarly, for a given gap width, finer hairs yield greater leakiness at a $Re$ of approximately 0.5, whereas this difference is only apparent at narrow gap widths at higher $Re$ (Fig. 10B).

Therefore, both physical and mathematical models show that reducing $G/D$ can lower leakiness at $Re \geq 10^{-2}$, although the $G/D$ below which this effect occurs can be quite small at $Re \geq 0.5$. As mentioned above, $G/D$ can also affect the leakiness of arrays of hairs operating at $Re \leq 10^{-2}$ if they move relative to a wall.

### What are the consequences of larger-scale flow around a whole appendage?

Leonard (1992) observed that the leakiness of his comb-like models (Fig. 8C) varied
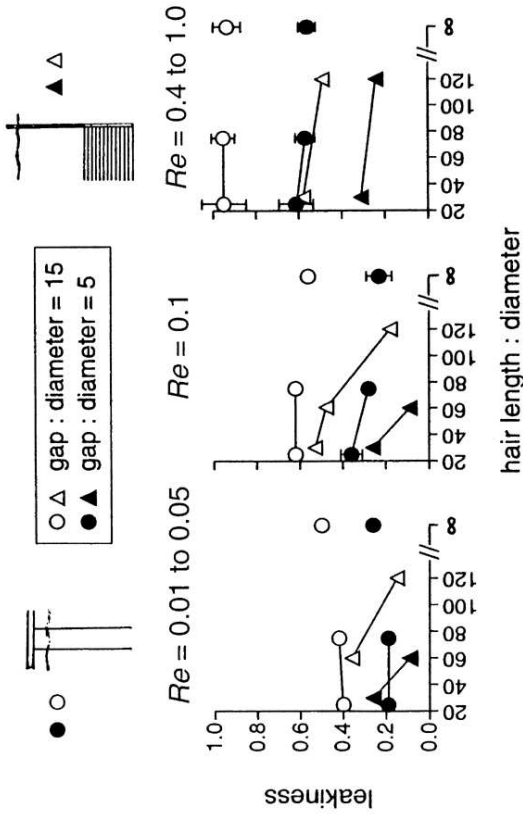


Fig. 9. Leakiness of various models as a function of hair length:diameter ratio. Open symbols represent models with a $G/D$ of 15; filled symbols represent models with a $G/D$ of 5; circles represent a pair of cylinders (Fig. 8A,B) at $Re$ of 0.01, 0.1 and 1 ($\infty$ indicates cylinders that were 'infinitely' long, extending from the floor of the tank to the top of the fluid) (B. A. Best, C. Loudon and M. A. R. Koehl, in preparation); triangles represent the comb-like models (Fig. 8D) of Hansen and Tiselius (1992) at $Re$ of 0.05, 0.1 and 0.4. Error bars, which indicate one standard deviation (s.d., $N=3–5$), are shown for the data of B. A. Best, C. Loudon and M. A. R. Koehl (in preparation) (although in some cases the standard deviations are smaller than the circles used to indicate the mean values); no standard deviations were reported by Hansen and Tiselius.

with time even though they were towed at steady velocities. He reported that the fluctuations in flow between hairs occurred as vortices were shed by the whole comb, and that the temporal and spatial pattern of this fluctuating leakiness depended not only on $G/D$ but also on the $Re$ of the whole array. Whether such fluctuating leakiness affects the performance of filters, gills or wings remains to be determined. Nonetheless, Leonard's work illustrates the importance of considering the higher-$Re$ flow around whole appendages even if our focus is on the details of the low-$Re$ flow around individual hairs.

## Physical models of copepod second maxillae

In order to explore how the morphology and motion of copepod M2s affect the water flow through the appendages, we built geometrically similar physical models (Fig. 8F) of the M2s of three species: *C. furcatus, E. pileatus* and *T. stylifera* (Fig. 6). The dimensions of the models (which were 48–57 mm long) were based on morphometric analyses of light micrographs and scanning electron micrographs of the M2s of the animals (M. A. R. Koehl, unpublished data). Each pair of model M2s was mounted on a wall (to simulate the body surface) in a tank of mineral oil (1 m×1 m×0.55 m) and was flapped to mimic the fling-and-squeeze of a copepod (Fig. 5) at $Re$ of 1, $10^{-1}$ and $10^{-2}$ (all Reynolds numbers in this discussion of M2s are based on the diameter of the setae). A plane (parallel to the length and normal to the width of the M2s) was illuminated through a slit with fiber-optic lamps (Cole Parmer no. 9741) and the fluid was marked with neutrally buoyant particles (*Artemia* cysts). Video records were made of the motion of the models and the marker particles and were digitized using a Peak Performance Video Motion Analysis System (version 5.1.0). These data were used to calculate the velocity of the fluid relative to the appendage (details described in M. A. R. Koehl and J. Jed, in preparation).

Examples of fluid velocities relative to the model M2s of *C. furcatus* ($Re=1$) and *T. stylifera* ($Re=10^{-2}$) are shown in Fig. 11. The differences between the flow patterns relative to the leaky appendage whose setae operate at a $Re$ of 1 and the paddle-like appendage whose hairs move at a $Re$ of $10^{-2}$ is striking. As illustrated by the vectors relative to the M2 of *T. stylifera* (Fig. 11), particles move slowly towards the tips of the setae of our model M2s at a $Re$ of $10^{-2}$; Price and Paffenhöfer (1986) have described similar particle motions near the M2s of copepods feeding at that $Re$.

Fluid velocity ($U_{rel}$) through the model appendage at some position along its length was divided by the speed ($U_{M2}$) at which the appendage was traveling at that position to yield a measure of the relative flow through the appendage. Since fluid velocity through the middle of a gap between hairs is a good predictor of leakiness (B A. Best, C. Loudon and M. A. R. Koehl, in preparation), high values of $U_{rel}/U_{M2}$ indicate sieve-like behavior and low values indicate paddle-like function. I will present below a few examples of the questions that can be answered by measuring the effects on $U_{rel}/U_{M2}$ of manipulations of the morphology or kinematics of physical models such as these.

What are the consequences of changing the $Re$ (i.e. the size or speed) at which the setae of the M2s of a copepod operate? As illustrated in Fig. 12, the coarse-meshed M2s of *C.*



A



B

Fig. 10. Leakiness of comb-like physical models (Fig. 8C,D). (A) Leakiness plotted as a function of $G/D$ for the models of Hansen and Tiselius (1992) (indicated by triangles) and of Leonard (1992) (indicated by circles). Black symbols represent $Re$ of about 40 ($Re$: triangles, 40; circles, 37); grey symbols represent $Re$ of about 3 ($Re$: triangles, 2.9 and 3.8; circles, 4). and open symbols represent $Re$ of 0.2. (B) Leakiness plotted as a function of gap width (in mm) for the models of Hansen and Tiselius (1992) composed of cylinders that were slim (0.5 mm diameter; represented by open circles) or thick (2.0 mm diameter; represented by black triangles). The $Re$ given above each graph is a rough approximation (in the left-hand graph, $Re$: open circles, 0.7, filled triangles, 0.4; in the middle graph, $Re$: circles, 2.2, triangles, 2.9; in the right-hand graph, $Re$: circles, 10.1, triangles, 7.5).
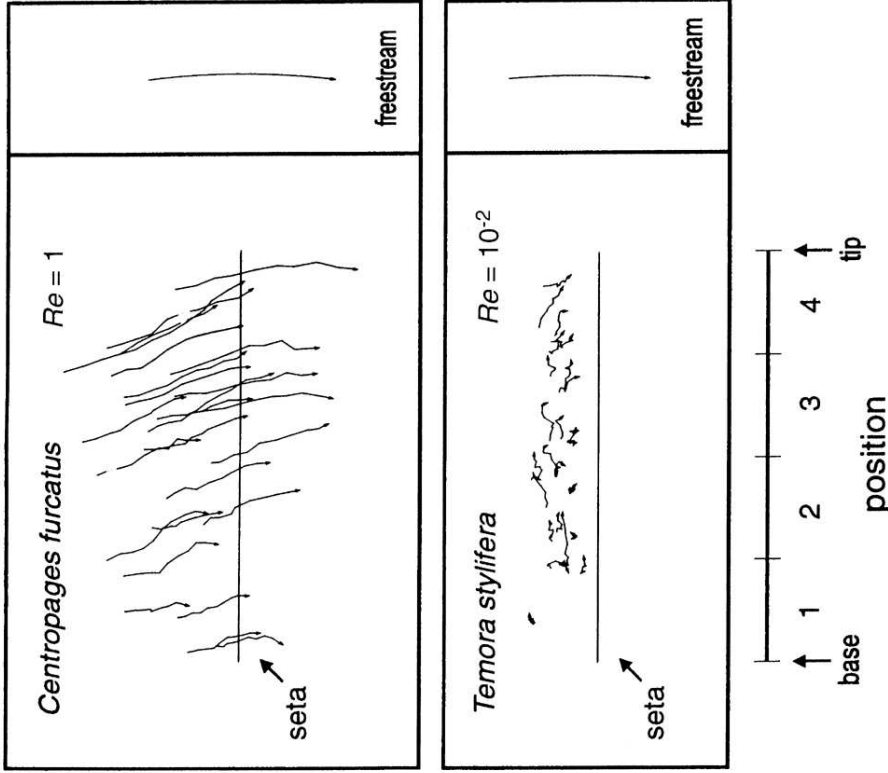
Fig. 10

Fig. 11. Velocities of marker particles relative to a marked seta on a dynamically scaled physical model (described in the text and Fig. 8F) of a C. furcatus M2 (A) and of a T. stylifera M2 (B) during fling motions (Fig. 5B,C). 'Freestream' indicates the velocity relative to the tip of the moving seta of the stationary fluid in the tank. The seta was divided into four regions (indicated by the scale at the bottom of the figure) and the velocity data for each section were pooled to generate graphs such as those in Figs 12 and 14.
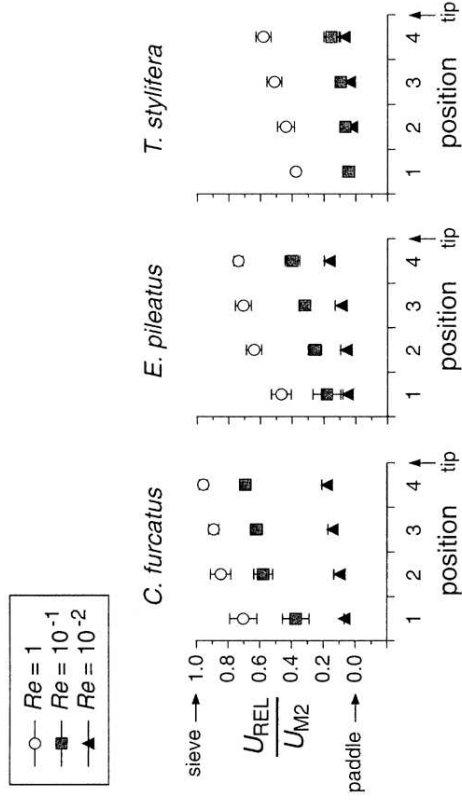


Fig. 12. Fluid movement through models of the M2s of C. furcatus (left-hand graph), E. pileatus (middle graph) and T. stylifera (right-hand graph). Fluid velocity ($U_{rel}$) through a model appendage at some point along its length was divided by the speed ($U_{M2}$) at which the appendage was traveling at that point to yield a measure of the relative flow through the appendage ($U_{rel}/U_{M2}$). The mean values of $U_{rel}/U_{M2}$ for each section of a model (see Fig. 11 for an explanation of positions 1, 2, 3 and 4) are plotted for models run at $Re$ of $10^{-2}$ (black triangles), $10^{-1}$ (grey squares) and 1 (open circles). Error bars indicate one standard deviation ($N$=3–12). Kruskal-Wallis tests were used to determine whether the values of $U_{rel}/U_{M2}$ at each position for each species were significantly different between $Re$ ($P<0.05$).

sieve-like behavior occurs is higher for the fine-meshed species than for the more coarsely meshed species.

E. pileatus are plastic in their feeding behavior and can change the $Re$ at which their M2s operate. For example, they catch particles with single or multiple fling-and-squeeze motions at $Re$ of the order of $10^{-2}$, but reject unwanted material at $Re$ of $10^{-1}$ (Koehl and Strickler, 1981; Price and Paffenhöfer, 1986; M. A. R. Koehl and G.-A. Paffenhöfer, unpublished data). Our model experiments indicate that a change in $Re$ between $10^{-2}$ and $10^{-1}$ can produce a large change in leakiness for E. pileatus M2s (Fig. 12) (Koehl and Strickler, 1981). Indeed, microcinematographic observations of dye motions near the M2s of E. pileatus show that little water moves through the M2s during the various feeding motions (Koehl and Strickler, 1981; Koehl, 1993; M. A. R. Koehl and G.-A. Paffenhöfer, unpublished data), whereas water flows readily through the M2s during the faster rejection, thereby pushing the unwanted material away from the animal as explained in Fig. 13 (Koehl and Strickler, 1981). E. pileatus illustrates that an animal's hairy appendage is not constrained by its morphology to be just a paddle or just a sieve if it can change its speed across the $Re$ range where the transition in leakiness occurs. In contrast, if a T. stylifera were to speed up its M2s to an $Re$ of $10^{-1}$, they would still operate as paddles (Fig. 12) because the leakiness transition occurs at higher $Re$ for this fine-meshed species.

What are the consequences to leakiness of differences in the morphology of the M2s?

furcatus (which normally operate at a $Re$ of approximately 1 and are sieve-like) can function as paddles if made to move at a $Re$ of $10^{-2}$, while the fine-meshed M2s of T. stylifera (which normally operate at a $Re$ of approximately $10^{-2}$ and are paddle-like) can leak like sieves if moved at a $Re$ of 1. However, the comparison of the three species shown in Fig. 12 reveals that the $Re$ range across which the transition from paddle-like to
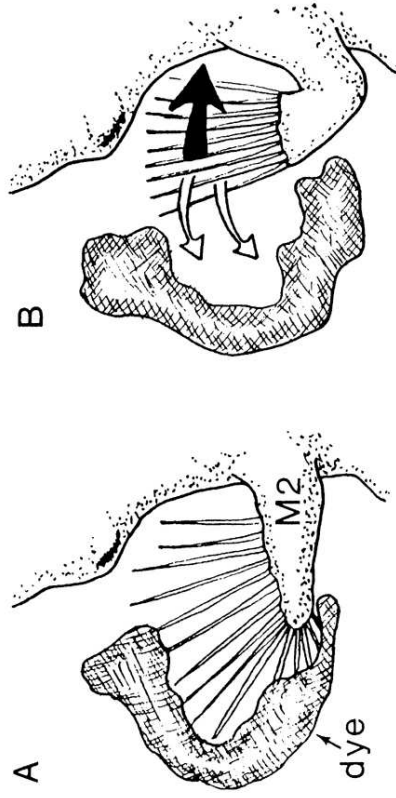
Fig. 13. Diagram of the rejection motion of the M2s of *E. pileatus* (diagrams based on tracings from a film of a feeding *E. pileatus* in Koehl and Strickler, 1981). (A) The copepod scrapes its M2s along the body surface and collects the unwanted material on the backs of the M2s. (B) After pushing the material away from the body, the M2s rapidly squeeze (black arrow) towards the body at an $Re$ of $2\times10^{-2}$ (Koehl and Strickler, 1981). The M2s are leaky enough at $Re=10^{-2}$ for water to move (white arrows) between the setae of the M2s, thereby pushing the unwanted material away. The rejected material is then carried off in the feeding current produced by the appendages indicated in Fig. 5A.
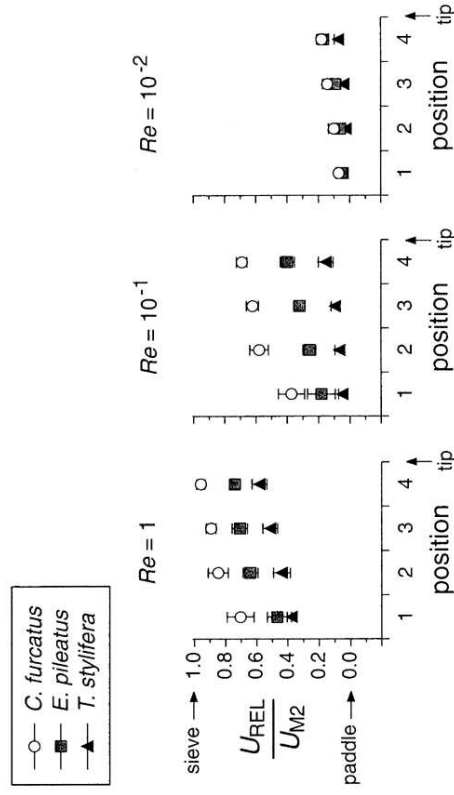


Fig. 14. Fluid movement through models of the M2s of *C. furcatus* (open circles), *E. pileatus* (grey squares) and *T. stylifera* (black triangles). The mean values of $U_{rel}/U_{M2}$ for each section of a model (see Fig. 11 for an explanation of positions 1, 2, 3 and 4) are plotted for models run at $Re$ of 1 (left-hand graph), $10^{-1}$ (middle graph) and $10^{-2}$ (right-hand graph). Error bars indicate one standard deviation ($N=3$–12). Kruskal-Wallis tests were used to determine whether the values of $U_{rel}/U_{M2}$ at each position for each $Re$ were significantly different between species ($P<0.05$).

Our model experiments show that the coarser the mesh of the M2, the higher the $U_{rel}/U_{M2}$ of the flow through it at $Re$ of 1 or $10^{-1}$ (Fig. 14). However, at $Re$ of $10^{-2}$, mesh coarseness has no significant effect on leakiness. Hence, once again we see that whether or not morphology affects flow through an array of hairs depends on $Re$.

## Conclusions

Many animals from different phyla use appendages composed of arrays of small hairs ($Re$ of $10^{-5}$ to 10) to catch food or molecules from the surrounding water or air and to locomote through or propel fluid. The performance of these various functions depends on the fluid motion around and through the appendages. Physical and mathematical modeling, performed in conjunction with kinematic and morphometric studies of hairy legs on real animals, have revealed a number of patterns in how the flow through arrays of hairs depends on their structure and behavior.

Rows of hairs operating at very low $Re$ function as paddles (i.e. little fluid moves between adjacent hairs), whereas those at $Re$ near 1 function like leaky sieves. The $Re$ range through which the transition in leakiness occurs depends on the geometry of the appendage.

How does the morphology of a row of hairs affect its leakiness? Increasing the gap:diameter ratio ($G/D$) of the array has little effect on leakiness at $Re\leq10^{-2}$, unless the array is moved relative to a nearby wall. In contrast, at $Re$ of $10^{-2}$ and $10^{-1}$, leakiness can be greatly increased if gaps are widened relative to hair diameters. However, if $Re$ is 1 or

10, gap width has little effect on leakiness unless $G/D$ is already very small. This example illustrates that there can be scope for morphological change without performance consequences in one range of $Re$, while in another $Re$ range there can be pronounced functional shifts as a consequence of the same structural alteration. Furthermore, a particular morphological change can have the *opposite* consequences at different $Re$. For example, increasing the number of hairs in a row decreases leakiness if $Re$ is less than 1, but increases leakiness if $Re$ is greater than 1.

How do the kinematics of appendage motion affect leakiness? If an animal whose hairs operate at very low $Re$ ($Re\leq10^{-2}$) changes the speed of hair motion, there is no effect on leakiness (although, of course, the absolute speed at which fluid moves through the gap is changed). In contrast, changes in the speed of motion of hairs operating at $Re>10^{-2}$ can produce large changes in leakiness. The coarser the mesh of the appendage, the lower the $Re$ at which this transition between paddle-like and sieve-like function occurs. In contrast, the behavior of moving the appendage closer to a wall increases the leakiness of hairs operating at $Re\leq10^{-2}$, whereas at higher $Re$ this behavior has no effect. These examples illustrate that different behaviors (i.e. modifying speed *versus* altering distance from a wall) must be used at different $Re$ to change leakiness.

These results have interesting implications if we consider the consequences of changing the size (and therefore changing the $Re$) of hair-bearing appendages, either during the growth of an individual or during the evolution of a lineage. Different types of

behaviors and morphological features can affect performance at different sizes; therefore, which structural and behavioral characters are subject to natural selection might be size-dependent. Furthermore, a simple change in size can lead to a novel function without requiring the development of a novel structure (in this example, we see that it is physically possible for an appendage that was a paddle at smaller size to acquire the ability to filter). Kingsolver and Koehl (1985) have discussed the the evolutionary implications of novel functions resulting from simple size changes.

Our experiments have also revealed some practical issues that should be kept in mind by anyone studying the fluid mechanics of hairs operating at $Re \leq 10^{-2}$. For mathematical models of appendages (which are of finite length and which flap near the surface of an animal's body), the assumption of an unbounded fluid will lead to an underestimation of leakiness, and the use of two-dimensional analyses will lead to an overestimation. For physical models moved through a tank of practical dimensions, the walls of the tank will increase the flow relative to the model. Although this effect is desirable when modeling appendages that move near body surfaces, it may pose problems when modeling organisms swimming in an unbounded fluid. Furthermore, even though suspension-feeding appendages may look like fibrous filters, the mechanism of particle capture by those of very low leakiness may not be filtration, but rather may depend on the movement of the water surrounding the particle.

## References

ALCARAZ, M., PAFFENHÖFER, G.-A. AND STRICKLER, J. R. (1980). Catching the algae: A first account of observations on filter-feeding calanoids. *Am. Soc. Limnol. Oceanogr. spec. Symp.* **3**, 241–248.

ATEMA, J. (1985). Chemoreception in the sea: Adaptations of chemoreceptors and behavior to aquatic stimulus conditions. *Soc. exp. Biol. Symp.* **39**, 387–423.

BERG, H. C. AND PURCELL, E. M. (1977). Physics of chemoreception. *Biophys. J.* **20**, 193–217.

BRAIMAH, S. A. (1987). Pattern of flow around filter-feeding structures of immature *Simulium bivittatum* Malloch (Diptera: Simuliidae) and *Isonychia campestris* McDunnough (Ephemeroptera: Oligoneuridae). *Can. J. Zool.* **65**, 514–521.

CHEER, A. Y. L. AND KOEHL, M. A. R. (1987a). Paddles and rakes: Fluid flow through bristled appendages of small organisms. *J. theor. Biol.* **129**, 17–39.

CHEER, A. Y. L. AND KOEHL, M. A. R. (1987b). Fluid flow through filtering appendages of insects. *IMA J. Math. appl. Med. Biol.* **4**, 185–199.

CHILDRESS, S., KOEHL, M. A. R. AND MIKSIS, M. (1987). Scanning currents in Stokes flow and the efficient feeding of small organisms. *J. Fluid Mech.* **177**, 407–436.

COWLES, T. J. AND STRICKLER, J. R. (1983). Characterization of feeding activity patterns in the planktonic copepod *Centropages typicus* Kroyer under various food conditions. *Limnol. Oceanogr.* **28**, 106–115.

CRAIG, D. A. AND CHANCE, M. M. (1982). Filter feeding in larvae of Simuliidae (Diptera: Culicomorpha): Aspects of functional morphology and hydrodynamics. *Can. J. Zool.* **60**, 712–724.

DAVIES, C. N. (1973). *Air Filtration*. New York: Academic Press.

ELLINGTON, C. P. (1975). Non-steady-state aerodynamics of the flight of *Encarsia formosa*. In *Swimming and Flying in Nature*, vol. 2 (ed. T. Y.-T. Wu, C. J. Brokaw and C. Brennan), pp. 783–796. New York: Plenum.

FUCHS, N. A. (1964). *The Mechanics of Aerosols*. Oxford: Oxford University Press.

FUTRELLE, R. P. (1984). How molecules get to their detectors: The physics of diffusion of of insect pheromones. *Trends Neurosci.* **7**, 116–120.

GERRITSEN, J. AND PORTER, K. G. (1982). The role of surface chemistry in filter feeding by zooplankton. *Science* **216**, 1225–1227.

HANSEN, B. AND TISELIUS, P. (1992). Flow through the feeding structures of suspension feeding zooplankton: A physical model approach. *J. Plankton Res.* **14**, 821–834.

KINGSOLVER, J. G. AND KOEHL, M. A. R. (1985). Aerodynamics, thermoregulation and the evolution of insect wings: Differential scaling and evolutionary change. *Evolution* **39**, 488–504.

KOEHL, M. A. R. (1981). Feeding at low Re by copepods. *Lect. Math. Life Sci.* **14**, 89–117.

KOEHL, M. A. R. (1983). The morphology and performance of suspension-feeding appendages. *J. theor. Biol.* **105**, 1–11.

KOEHL, M. A. R. (1984). Mechanisms of particle capture at low Reynolds numbers: Possible modes of selective feeding. In *Trophic Interactions in Aquatic Ecosystems* (ed. D. L. Meyers and J. R. Strickler), pp. 135–166. Boulder, CO: Westview Press.

KOEHL, M. A. R. (1993). Hairy little legs: Feeding, smelling and swimming at low Reynolds numbers. *Contemp. Math.* **141**, 33–64.

KOEHL, M. A. R., CHEER, A. Y. L. AND PAFFENHÖFER, G.-A. (1984). Water flow around and particle capture by bristled appendages of zooplankton. *EOS Trans. Am. Geophys. Un.* **60**, 925.

KOEHL, M. A. R. AND STRICKLER, J. R. (1981). Copepod feeding currents: Food capture at low Reynolds number. *Limnol. Oceanogr.* **26**, 1062–1073.

KOO, J.-K. AND JAMES, D. F. (1973). Fluid flow around and through a screen. *J. Fluid Mech.* **60**, 513–538.

LABARBERA, M. (1984). Feeding currents and particle capture mechanisms in suspension feeding animals. *Am. Zool.* **24**, 71–84.

LAWS, E. M. AND LIVESEY, J. L. (1978). Flow through screens. *A. Rev. Fluid Mech.* **10**, 247–266.

LEONARD, A. B. P. (1992). The biomechanics, autecology and behavior of suspension-feeding in crinoid echinoderms. PhD dissertation, University of California, San Diego.

LOUDON, C. (1990). Empirical test of filtering theory: Particle capture by rectangular-mesh nets. *Limnol. Oceanogr.* **35**, 143–148.

LOUDON, C., BEST, B. A. AND KOEHL, M. A. R. (1994). When does motion relative to neighboring surfaces alter the flow through arrays of hairs? *J. exp. Biol.* **193**, 133–254.

MOORE, P. A., ATEMA, J. AND GERHARDT, G. A. (1991). Fluid dynamics and microscale chemical movement in the chemosensory appendages of the lobster, *Homarus americanus*. *Chem. Senses* **16**, 663–674.

MORRIS, M. J., KOHLHAGE, K. AND GUST, G. (1990). Mechanics and energetics of swimming in the small copepod *Acanthocyclops robustus* (Cyclopoida). *Mar. Biol.* **107**, 83–91.

MURRAY, J. D. (1977). Reduction of dimensionality in diffusion processes: Antenna receptors of moths. In *Lectures on Nonlinear-Differential-Equation Models in Biology*, pp. 83–127. Oxford: Oxford University Press.

PAFFENHÖFER, G.-A., STRICKLER, J. R. AND ALCARAZ, M. (1982). Suspension-feeding by herbivorous calanoid copepods: A cinematographic study. *Mar. Biol.* **67**, 193–199.

PRICE, H. J. AND PAFFENHÖFER, G.-A. (1984). Effects of feeding experience in the copepod *Eucalanus pileatus*: A cinematographic study. *Mar. Biol.* **84**, 35–40.

PRICE, H. J. AND PAFFENHÖFER, G.-A. (1986). Capture of small cells by the copepod *Eucalanus elongatus*. *Limnol. Oceanogr.* **31**, 189–194.

PRICE, H. J., PAFFENHÖFER, G.-A. AND STRICKLER, J. R. (1983). Modes of cell capture in calanoid copepods. *Limnol. Oceanogr.* **28**, 116–123.

RUBENSTEIN, D. I. AND KOEHL, M. A. R. (1977). The mechanisms of filter feeding: Some theoretical considerations. *Am. Nat.* **111**, 981–994.

RUPPERT, E. E. AND BARNES, R. D. (1994). *Invertebrate Zoology*. Sixth edition. Fort Worth, TX: Saunders College Publishing.

RUSSELL-HUNTER, W. D. (1979). *A Life of Invertebrates*. New York: Macmillan Publishing Co., Inc.

SCHMIDT, B. C. AND ACHE, B. W. (1979). Olfaction: Responses of a decapod crustacean are enhanced by flicking. *Science* **205**, 204–206.

SHIMETA, J. AND JUMARS, P. (1991). Physical mechanisms and rates of particle capture by suspension feeders. *Oceanogr. mar. Biol. A. Rev.* **29**, 191–257.

SILVESTER, N. R. (1983). Some hydrodynamic aspects of filter feeding with rectangular-mesh nets. *J. theor. Biol.* **103**, 265–286.

SPIELMAN, L. A. AND GOREN, S. L. (1968). Model for predicting pressure drop and filtration efficiency in fibrous media. *Env. Sci. Technol.* **2**, 279–287.

STRICKLER, J. R. (1984). Sticky water: A selective force in copepod evolution. In *Trophic Interactions in Aquatic Ecosystems* (ed. D. L. Meyers and J. R. Strickler), pp. 187–239. Boulder, CO: Westview Press.

TAMADA, K. AND FUJIKAWA, H. (1957). The steady two-dimensional flow of viscous fluid at low Reynolds numbers passing through an infinite row of equal parallel circular cylinders. *Q. J. Mech. appl. Math.* **10**, 425–432.

TAYLOR, G. I. AND BATCHELOR, G. K. (1949). The effects of wire gauze on small disturbances in uniform stream. *Q. J. Mech. appl. Math.* **2**, 1–29.

VANDERPLOEG, H. A. AND PAFFENHÖFER, G.-A. (1985). Modes of algal capture by the freshwater copepod *Diaptomus sicilis* and their relation to food-size selection. *Limnol. Oceanogr.* **30**, 871–885.

VOGEL, S. (1983). How much air passes through a silkmoth's antenna? *J. Insect Physiol.* **29**, 597–602.